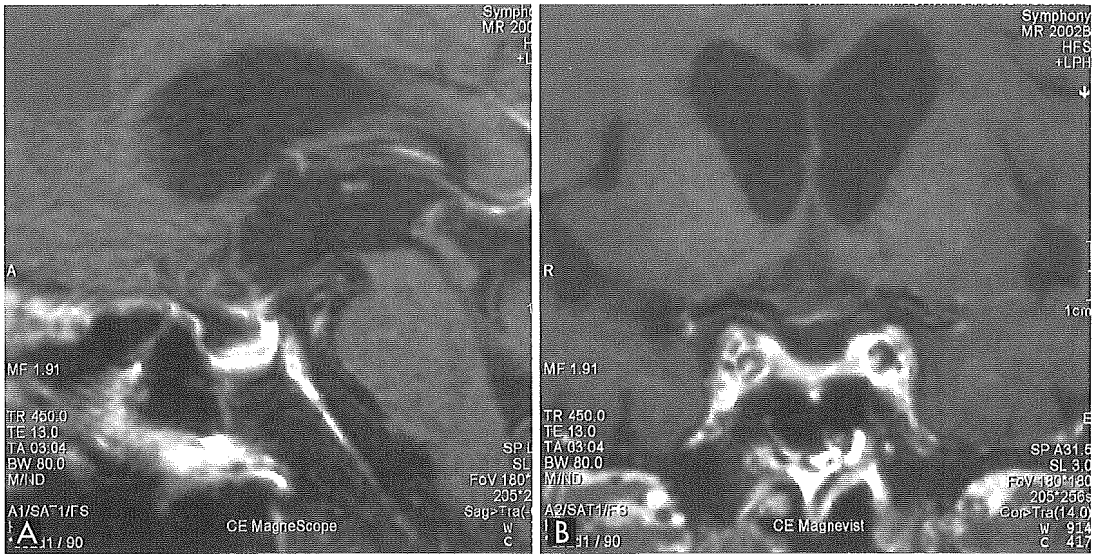

Fig. 5 Gadolinium-enhanced MRI after radiationtherapy (A: sagittal image, B: coronal image). The tumor remains stable without evident growth.

Table Summary of reported 5 cases and present case of craniopharyngioma

Author	Age/Sex	Symptoms	Treatment	Progree
Witt	70/F	visual impairment	transcranial (pterional)	visual function improved
Russell	72/M	visual impairment headache, distabance of consciousness	cyst aspiration	dead
Lederman	82/F	visual impairment hypopituitarism, DI (-)	transsphenoidal RT (59.4Gy)	visual function improved
Sekiya	74/F	visual impairment NPH	VP shunt transcranial (pterional)	visual function improved
	79/F	visual impairment	transcranial (pterional)	dead
Present case	80/F	visual impairment	transcranial (interhemispheric) RT (54Gy)	visual function improved

DI: diabetes inspidus NPH: normal pressure hydrocephalus RT: radiotherapy

し得た高齢者頭蓋咽頭腫例をまとめたが，高齢者においては初発症状として下垂体機能不全は少なく，全例視力視野障害で発症し，小児例，成人例の症状とは異なっていた．また，関谷ら[15]の症例では，本例の如く白内障と誤診され，高齢者に特有の診断上の問題点と考えられた．70歳以上の高齢者の手術適応に関しては今回渉猟し得た症例から考察すると，術後に肺炎など様々な全身合併症を伴い，6例中2例[14,15]が術後合併症で死亡していた．このことから，高齢者においては手術に慎重であるべきで，手術施行の際には熟達した術者が執刀すべきと考えられた．

Tableに示した6例での手術方法は，cyst aspiration，開頭摘出術，経蝶形骨洞手術が行われている．cyst aspirationは低侵襲な方法ではあるが，短期間に高率に再貯留するという報告があり[6]，aspiration後直ちに，腫瘍摘出術，放射線療法，ガンマナイフなどを行う必要があると考えられる[3,6,11,12]．また，Lederman ら[9]の症例のように可能であれば経蝶形骨洞手術を選択し，手術侵襲を軽減することも考慮すべきと考えられる．しかし，経蝶形骨洞手術は，腫瘍が鞍内に存在する場合に

はよい方法と考えられるものの，実際にはわれわれの症例の如く正常下垂体が鞍底に存在する例や腫瘍が鞍上部に進展する例には経蝶形骨洞手術の適応にはならないと考えられる．開頭時のアプローチの選択に関しては，術者の技術，施設の方針に基づき症例ごとに決定されるべきと考えられる．

全年齢層を対象とした開頭摘出術の治療成績[4-7,17]をみると，Yasargilら[17]の144例の報告では133例で開頭手術が行われ，全摘出率は90%，術後合併症は16.7%，死亡率は2.1%（2例）であった．この2例とも視床下部からの出血が死因であった．またFahlbuschら[6]の168例の報告では，113例に開頭手術を行っており，全摘出は41.5%，亜全摘出は30%，部分摘出は29.2%であった．術後合併症は13.2%，死亡率は1.1%（1例）であった．死亡した1例は心疾患の既往歴があり，術後2日目に心停止により死亡した．これまで報告のあった症例をまとめる[4-7,17]と術後の内分泌機能温存，記名力障害の回避を目的に，視床下部に癒着した部分は無理に摘出することなく意図的に残存させ，視床下部機能を温存することにより良好な経過を得ることができているようである．このことが，頭蓋咽頭腫，特に高齢者の手術における要点と考えられた．

また残存腫瘍に対してはガンマナイフ治療[1,3,11,13]や放射線療法の有効性が報告されている[12,13]．ガンマナイフ治療の成績をみると，Amendolaら[1]の報告では39.2カ月の追跡で再発例はなく，Chungら[3]の31例の報告では，36カ月の追跡では4例（13%）に再発を認めている．一方，放射線外照射の成績をみると，Rajanら[12]の173例の報告では非全摘出術例148例に対し術後放射線療法を行っており，再発率は15%であった．放射線療法を行わない非全摘出例の再発率は33～69%[4-6,17]と報告されており，残存腫瘍に対し放射線療法を行うことで再発をある程度抑えることができるものと考えられる．しかしながら放射線外照射は照射後の認知症（痴呆）発生の問題もあり[2,10]，照射野を狭くするなどの考慮が必要である．当院で術後残存腫瘍に対してガンマナイフを施行した症例は6例であるが，6例中2例が腫瘍の再増大を認め，ガンマナイフ後9カ月および3年で再手術を行っている．再発例はいずれも視交叉近傍に腫瘍が残存したため線量を低く抑えざるを得なかった症例であった．本例でも残存腫瘍は視交叉下面に接しており，ガンマナイフ治療では十分に照射することが難しいと考えられた[13]．高齢者ではあったが再発の阻止に必要な線量は50～60 Gy[1,13,14]と報告されており，原体照射を行うことで照射野を絞り込み54 Gyの放射線治療を施行した．

Ⅳ. 結　語

良好な術後経過を得た80歳，頭蓋咽頭腫の稀な1例を報告した．高齢者頭蓋咽頭腫は視力視野障害で発症することが多く，視機能の障害は患者のADLを極度に低下させることから，高齢者であっても摘出術を考慮すべきであると考える．ただし，手術に際して良好な術後経過を得るためには，術後の間脳下垂体機能障害回避のため下垂体柄に癒着した部分は無理せず，場合によってはその部分のみを意図的に残し機能を温存することが肝要であると考えられる．

文　献

1) Amendola BE, Wolf A, Coy SR, Amendola MA：Role of radiosurgery in craniopharyngioma：A preliminary report. Med Pediatr Oncol **41**：123-127, 2003
2) 浅井昭雄，松谷雅生，松田忠義，田中良明，船田信顕：放射線性脳萎縮の臨床組織学的検討．癌の臨床 **35**：1325-1329, 1989
3) Chung WY, Pan DH, Shiau CY, Guo WY, Wang LW：Gamma knife radiosurgery for craniopharyngiomas. J Neurosurg **93**：47-56, 2000
4) Duff JM, Meyer FB, Ilstrup DM, Laws ER, Schleck CD, Scheithauer BW：Long-term outcomes for surgically resected craniopharyngiomas. Neurosurgery **46**：291-305, 2000
5) Effenterre RV, Boch AL：Craniopharyngioma in adults and children：A study of 122 surgical cases. J Neurosurg **97**：3-11, 2002
6) Fahlbusch R, Honegger J, Paulus W, Huk W, Buchfelder M：Surgical treatment of craniopharyngiomas：Experience with 168 patients. J Neurosurg **90**：237-250, 1999
7) Fischer EG, Welch K, Shillito J, Winston KR, Tarbell NJ：Craniopharyngiomas in children. J Neurosurg **73**：

534-540, 1990
8) Hoffman HJ,Silva MD,Humphreys RP,Drake JM,Smith ML,Blaser SI：Aggressive surgical management of craniopharyngiomas in children.J Neurosurg **76**：47-52, 1992
9) Lederman GS,Recht A,Loeffler JS,Dubuisson D, Kleefield J, Schnitt AJ：Craniopharyngioma in an elderly patient. Cancer **60**：1077-1080, 1987
10) 松谷雅生：老年者の脳腫瘍の治療－放射線療法－．老化と疾患 **7**：71-76, 1994
11) 大須浩二，小林達也，木田義久，田中孝幸，吉田和雄，長谷川俊典：小児頭蓋咽頭腫に対するガンマナイフ手術の長期効果．小児の脳神経 **26**：14-18, 2001
12) Rajan B, Ashley S, Gorman C, Jose CC, Horwish A, Bloom HJG, Marsh H, Brada M：Craniopharyngioma-long-term results following limited surgery and radiotherapy. Radiother Oncol **26**：1-10, 1993
13) Regine WF, Kramer S：Pediatric craniopharyngiomas：Long term results of combined treatment with surgery and radiation. Int J. Radiat Oncol Biol Phys **24**：611-617, 1992
14) Russell RWR,Pennybacker JB：Craniopharyngioma in the elderly. J Neurol Neurosurg Psychiatry **24**：1-13, 1961
15) 関谷徹治，伊藤勝博，赤坂健一，鈴木重晴：高齢者（70歳以上）頭蓋咽頭腫の2手術例．No Shinkei Geka **23**：699-703, 1995
16) Witt JA, MacCarty CS, Keating FR：Craniopharyngioma (pituitary adamantioma) in patients more than 60 years of age. J Neurosurg **12**：354-360, 1955
17) Yasargil MG, Curcic M, Kis M, Siegenthaler G, Teddy PJ, Roth P：Total removal of craniopharyngiomas. J Neurosurg **73**：3-11, 1990

Acta Neurochir (Wien) (2005) 147: 721–726
DOI 10.1007/s00701-005-0540-4

Acta Neurochirurgica
Printed in Austria

Clinical Article

Gamma knife surgery for brain metastases: indications for and limitations of a local treatment protocol

T. Serizawa[1], N. Saeki[2], Y. Higuchi[1], J. Ono[1], T. Iuchi[3], O. Nagano[2], and A. Yamaura[2]

[1] Department of Neurosurgery, Chiba Cardiovascular Center, Ichihara, Japan
[2] Department of Neurological Surgery, Graduate School of Medicine, Chiba University, Chiba, Japan
[3] Division of Neurological Surgery, Chiba Cancer Center, Chiba, Japan

Received June 4, 2004; accepted March 31, 2005; published online May 20, 2005

Summary

Objective. The purpose of this retrospective study was to evaluate results of a local treatment protocol using gamma knife surgery (GKS) for brain metastases without upfront whole brain radiation therapy (WBRT).

Methods. Results for 521 consecutive patients satisfying the following 3 criteria were analysed: 1) a maximum of 3 tumours with a diameter of 25 mm or more; 2) no prior WBRT; 3) no surgically inaccessible large (>30 mm) tumours. Large tumours were surgically removed and all smaller lesions were treated by GKS without upfront WBRT. New lesions, detected with follow-up MRI, were appropriately treated with repeat GKS. Overall survival (OS), neurological survival (NS), qualitative survival (QS) and new lesion-free survival (NLFS) curves were calculated and the prognostic values of covariates were obtained. OS and NS were compared according to tumour number.

Results. In total, 1023 separate sessions were required to treat 4562 lesions. The primary organs were lung in 369 patients, gastrointestinal tract in 70, breast in 33, urinary tract in 24, and others/unknown in 25. The median OS period was 9.0 months. On multivariate analysis, the significant prognostic factors for OS were found to be extracranial disease (risk factor: active), Karnofsky performance status (KPS) score (<70) and gender (male). NS and QS at one year were 85.6% and 73.0%, respectively. The only significantly poor prognostic factor for NS was carcinomatous meningitis. NLFS at 6 months was 68.9%. For both OS and NS, the differences between a few (≤3) and many (4–10) brain lesions were not significant (OS: $p = 0.3128$, NS: $p = 0.5509$). Patients with numerous (>10) tumours had a significantly poorer prognosis than those with ≤10.

Conclusion. Our protocol, aggressively applying GKS, provides excellent results in selected patients with ≤10 brain lesions and no carcinomatous meningitis.

Keywords: Brain metastasis; stereotactic radiosurgery; gamma knife surgery; whole brain radiation therapy.

Introduction

Excellent results have been reported using radiosurgery for a few small metastatic brain tumours resulting from various systemic cancers [2, 3, 5–7, 13]. However, most previous studies were small or multi-institutional and followed inhomogeneous management protocols, and few prospective randomised studies comparing radiosurgery alone and radiosurgery plus WBRT have been reported [2, 3, 5–7, 9, 14, 15]. Furthermore, they evaluated only OS, which depended mainly on the extracranial disease and pre-treatment KPS score. NS and QS should be considered in discussing the results of treating brain metastases. In this retrospective study, we carefully reviewed a very large series of results of GKS without upfront WBRT for brain metastases, treated according to the same protocol, at a single institute with special attention paid to NS and QS, and discuss the indications and limitations herein.

Patients and methods

Among 550 cases with brain metastases treated by GKS at Chiba Cardiovascular Center from January 1998 through December 2002, 521 consecutive patients who satisfied the following 3 criteria were enrolled: 1) a maximum of 3 tumours with a diameter ≥25 mm; 2) no prior WBRT; 3) no surgically inaccessible large (>30 mm) tumours. Patients with miliary cerebral dissemination (>25) were excluded in this study. All metastatic lesions were diagnosed on gadolinium-enhanced MRI (1.5 Tesla, Magnetom Vision, Siemens) with a 5-mm thickness and no gaps. At diagnosis of brain metastases, the primary physician evaluated

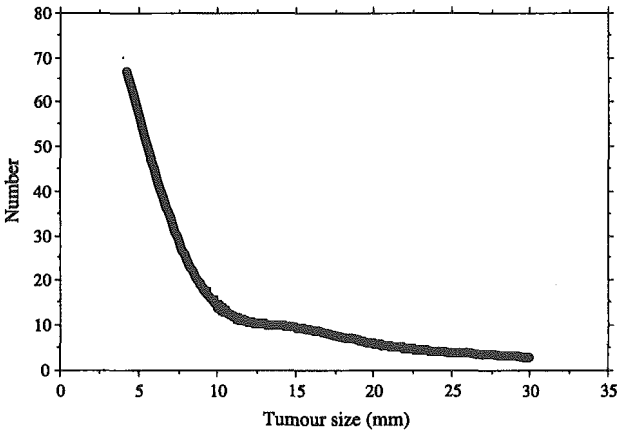

Fig. 1. Limits of lesion number and size for gamma knife surgery: The curve indicates a 3 Gy mean whole brain radiation dose calculated using the GammaPlan with 20 Gy (50%) peripheral doses. Within these limits, we assume that 25 tiny (8 mm), 10 small (14 mm) or 4 medium-sized (25 mm) lesions can be safely irradiated at a single GKS session

the status of extracranial disease using x-ray films, CT scanning and radionuclide scanning. According to the protocol of this study, large tumours (>30 mm) were surgically removed, and smaller lesions (≤30 mm) were treated by GKS without upfront WBRT. Additional GKS to the tumour bed was performed with 18–20 Gy when neurosurgeons judged the lesion to have been incompletely resected. New distant lesions detected by gadolinium-enhanced MRI were appropriately treated with repeat GKS, if the patient's condition allowed. For all GKS procedures, the mean whole brain radiation dose calculated with the Leksell GammaPlan™ (Elekta Instruments, Atlanta, GA) was kept below 3 Gy, thus preventing acute brain swelling, as previously reported [10, 11]. According to our criteria, if the lesions are scattered and similar in size, the upper simulated numerical limit is approximately 25 for tiny (8 mm), 10 for small (14 mm) and 3 for medium-sized (25 mm) lesions, with 20 Gy at the periphery, as presented in Fig. 1. Chemotherapy was administered by the primary physician.

Neurological and neuroradiological evaluations were performed every one to three months after initial GKS. Control of the GKS-treated lesion was defined as the absence of any significant increase in tumour diameter (<10%), as confirmed by axial or coronal MRI. To differentiate tumour recurrence from radiation injury, thallium-201 Chloride (Tl) SPECT was employed, as previously reported [12]. With these measurement methods, a high (>5.0) Tl index indicates tumour recurrence, a low (<3.0) index radiation injury. In lesions with an intermediate (≥3.0, ≤5.0) index, the Tl SPECT studies were repeated until the index exceeded 5.0 or was less than 3.0. Neurological death was defined as death due to all forms of intracranial disease, including tumour recurrence, carcinomatous meningitis, cerebral dissemination, and other unrelated intracranial disease. Impaired activity of daily life (ADL) was defined as an impaired neurological status as reflected by a Karnofsky performance status (KPS) score <70 (functionally dependent). A new lesion was defined as the appearance of a new brain metastasis at a site different from the original one.

The intervals from the date of initial referral to our center until the date of death (overall survival, OS), neurological death (neurological survival, NS), impaired ADL (qualitative survival, QS), and appearance of new distant lesions (new-lesion-free survival, NLFS) were calculated by the Kaplan-Meier method. The tumour-progression-free survival for all lesions treated with GKS was also analysed. Prognostic values of the individual covariates for OS, NS, QS and NLFS were obtained with the Cox proportional hazards model. The following 11 dichotomised covariates were entered: age (≥65 years versus <65 years); gender (male versus female); pre-treatment KPS score (≥70 versus <70); extracranial disease (controlled versus active); diagnostic timing of brain metastasis with primary site (synchronous versus metachronous); primary organ (lung cancer versus non-lung cancer); brain lesion number (>10 versus ≤10); maximum lesion size (≥25 mm versus <25 mm); presence of carcinomatous meningitis at initial MRI (yes versus no); chemotherapy (yes versus no) and craniotomy (yes versus no). Covariates revealed to be significant by univariate analyses were included in the multivariate model verified by stepwise methods in the final model. According to tumour number (a few: ≤3, many: 4–10, numerous: >10), OS and NS were also compared by logrank test. A probability value <0.05 was considered statistically significant.

Results

The distributions of dichotomised covariates are summarised in Table 1. In total, 1023 separate GKS

Table 1. *Distribution of patient characteristics*

Characteristics	Number of patients
Age (years)	
<65	252
≥65	269
Gender	
male	322
female	199
Extracranial disease	
controlled	68
active	453
Initial KPS score	
<70	94
≥70	427
Primary organ	
lung	367
non-lung	154
Brain lesion number	
≤10	433 (single 121)
>10	88
Maximum lesion size	
<25 mm	343
≥25 mm	178
Carcinomatous meningitis	
yes	45
no	476
Chemotherapy	
yes	148
no	373
Craniotomy	
yes	97
no	424
Diagnostic timing	
synchronous	358
metachronous	163

KPS Karnofsky performance status.

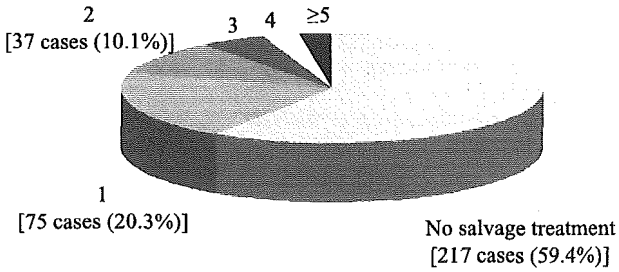

Fig. 2. Number of salvage treatments: There were zero salvage treatments by gamma knife surgery in 217 cases (59.4%), one in 74 (20.3%), two in 37 (10.1%), three in 19 (3.6%), and ≥5 in 19 (3.6%)

procedures were required to treat 4562 lesions. The median number of lesions treated by the initial GKS was 3, range 1 to 25. During follow-up, the number of GKS procedures averaged 1.7 ± 1.3, varying between 1 and 9 (Fig. 2), and the mean total number of lesions treated per patient with GKS was 8.9 ± 11.4, range 1 to 77. The mean calculated tumour volume was $1.0 \pm 2.8\,cm^3$. The minimum dose applied to the tumour margin was 13.3 to 33.3 Gy (mean ± SD 20.8 ± 2.4 Gy, median 20 Gy) with a 59.5% isodose contour (range 30–95%). The whole brain radiation dose was 0.1 Gy to 3.0 Gy (mean ± SD 1.2 ± 0.6 Gy, median 1.1 Gy). In 57 incompletely resected lesions of 97 operations (58.8%), the tumour bed was additionally irradiated with 18–20 Gy using GKS. The primary cancers were in the lung in 369 patients (72.1%), gastro-intestinal tract in 70 (13.4%), breast in 33 (6.3%), urinary tract in 24 (4.6%), and others/unknown in 25 (4.8%). The tumour-progression-free survival rates were 95.7% at one year and 91.1% at 2 years. The median OS period was 9.0 months (Fig. 3a). In multivariate analysis, significant prognostic factors for OS were active extracranial disease ($p < 0.0001$), low pre-treatment KPS score ($p < 0.0001$) and male gender ($p = 0.0028$), as shown in Table 2. NS and QS at one year were 85.6% and 73.0%, respectively (Fig. 3b, c). Of the 365 mortalities, 66 (18.1%) were attributed to neurological death. Causes of neurological death were carcinomatous meningitis in 26, cerebral

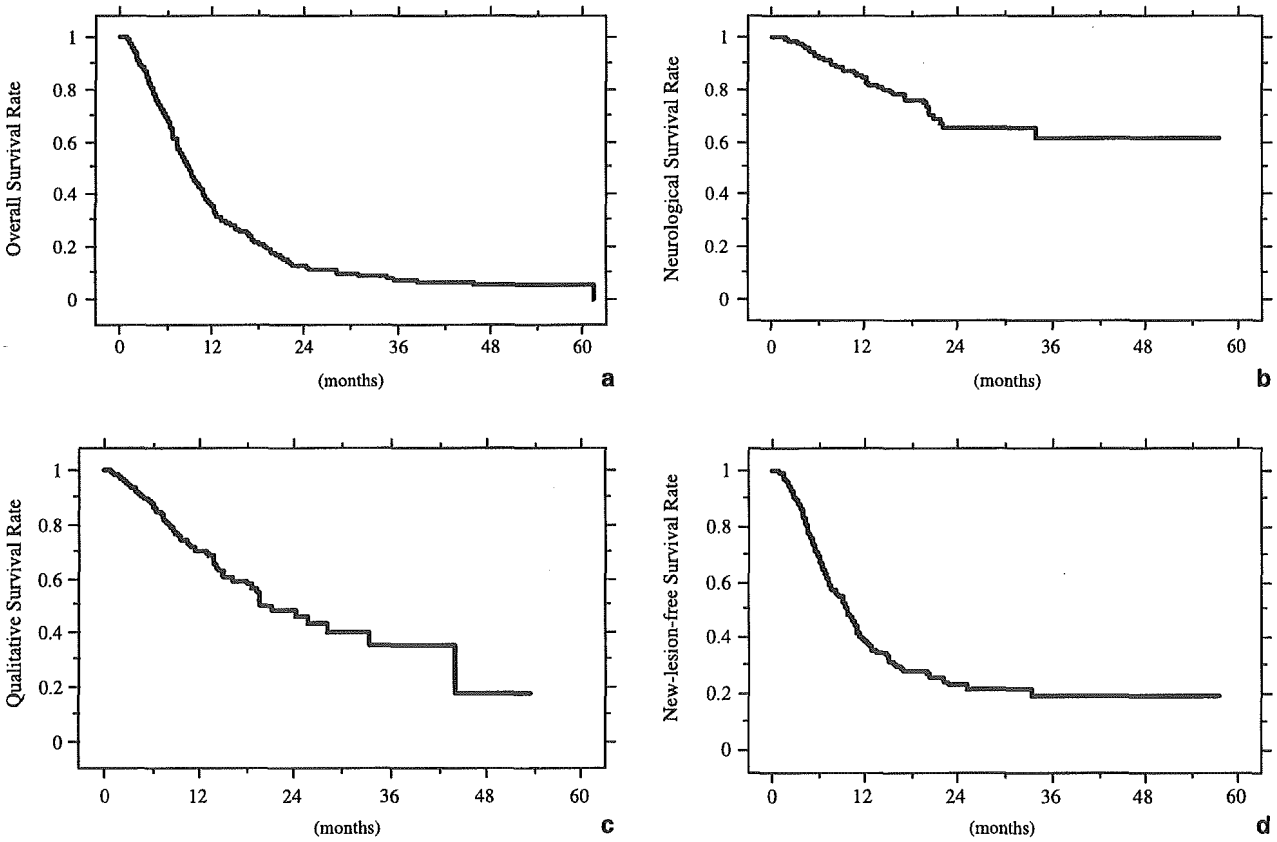

Fig. 3. (a) Overall survival: The overall survival (*OS*) curve is presented. The median OS period was 9.0 months. (b) Neurological survival: The neurological survival curve is shown. The neurological death free rate following GKS was 85.6% at one year. (c) Qualitative survival: The qualitative survival (*QS*) curve is presented. The functional-dependent-free rate was 73.3% at one year. (d) New-lesion-free survival: The new-lesion-free survival (*NLFS*) curve is shown. The NLFS rate was 68.9% at 6 months, 38.9% at 1 year

Table 2. *Prognostic variables for overall survival*

Variables	High risk group	P-value*	HR*	P-value**	HR**
Age	≥65	0.9995	1.000		
Gender	male	0.0027	1.389	0.0028	1.392
Extracranial disease	active	<0.0001	4.098	<0.0001	3.969
Initial KPS score	<70	<0.0001	1.845	<0.0001	1.864
Primary organ	non-lung	0.0242	1.290		
Brain lesion number	>10	0.0010	1.580		
Maximum lesion size	≥25 mm	0.2281	1.142		
Presence of CM	yes	0.0494	1.434		
Chemotherapy	no	0.1246	1.189		
Microsurgery	no	0.1214	1.225		
Diagnostic timing	synchronous	0.4133	1.098		

* Monovariate analysis, ** Multivariate analysis (Cox's proportional hazard final model), *HR* hazard ratio, *KPS* Karnofsky performance status, *CM* carcinomatous meningitis.

Table 3. *Prognostic variables for neurological survival*

Variables	High risk group	P value*	HR*	P value**	HR**
Age	<65	0.2631	1.339		
Gender	male	0.3039	1.314		
Extracranial disease	active	0.0113	2.577		
Initial KPS score	<70	0.1622	1.628		
Primary organ	non-lung	0.5436	1.186		
Brain lesion number	>10	0.0009	2.681		
Maximum lesion size	≥25 mm	0.2818	1.326		
Presence of CM	yes	<0.0001	8.013	<0.0001	8.013
Chemotherapy	no	0.3366	1.311		
Microsurgery	yes	0.9206	1.030		
Diagnostic timing	synchronous	0.4857	1.209		

* Monovariate analysis, ** Multivariate analysis (Cox's proportional hazard final model), *HR* hazard ratio, *KPS* Karnofsky performance status, *CM* carcinomatous meningitis.

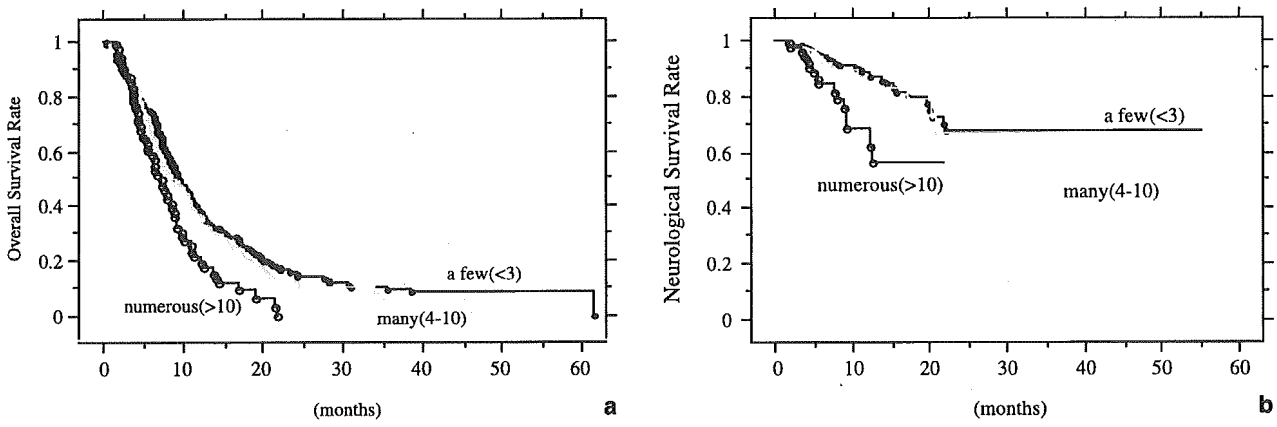

Fig. 4. Overall and neurological survival curves according to tumour number: (a) Overall survival curves according to tumour number: The difference between a few (≤3) and many (4–10) lesions was not statistically significant (p = 0.3128). The outcome of patients with numerous (>10) lesions was significantly poorer than that of those with a few (p = 0.0025) or many (p = 0.0144). (b) Neurological survival curves according to tumour number: Neurological survival curves according to tumour number are shown. The difference between a few (≤3) and many (4–10) lesions was not statistically significant (p = 0.5509). Patients with numerous (>10) lesions had a significantly poorer outcome than those with a few (p = 0.0017) or many (p = 0.0098)

dissemination in 18, recurrence of the treated lesion in 14, progression of an untreated lesion in 7 and other in 1. Among 105 cases with functional dependence due to brain lesions, the causes were radiation injury in 31, carcinomatous meningitis in 28, cerebral dissemination in 20, recurrence of the treated lesion in 16, progression of an untreated lesion in 9, and other in 1. The only significantly poor prognostic factor for NS was carcinomatous meningitis ($p<0.0001$), as depicted in Table 3. Extracranial active disease ($p=0.0008$), poor pre-treatment KPS score ($p=0.0002$) and carcinomatous meningitis ($p<0.0001$) were confirmed to be significant factors influencing QS in multivariate analysis. NLFS at 6 months was 68.9% (Fig. 3d). New lesions emerged more frequently in patients with active extracranial disease ($p=0.0017$) and numerous (>10) brain metastases ($p=0.0365$). OS and NS curves, according to tumour number, are shown in Fig. 4a and b, respectively. For both OS and NS, the differences between a few (≤3) and many (4–10) were not statistically significant (OS: $p=0.3128$, NS: $p=0.5509$), but the outcome of patients with numerous (>10) lesions was significantly poorer that of those with ≤10 (ON: $p=0.0144$, NS: $p=0.0017$).

Discussion

Patients with many (>4) lesions have been considered to have a poorer prognosis than those with a few (≤3). This study revealed the differences in OS and NS between a few (≤3) and many (4–10) to be statistically not significant and suggests that the limit of lesion numbers for GKS is around 10, as previously reported [10, 11]. GKS in a single session is limited not only by lesion number, but also lesion size. However, most earlier investigators focused solely on number [2, 3, 5–9, 13–15]. Both the number and the size of lesions affect the mean whole brain radiation dose, which provides information on the limits for GKS in a single session [10, 11]. With a mean skull radiation dose of 3 Gy or less, our calculations indicate 25 tiny (8 mm), 10 small (14 mm) or 4 medium-sized (25 mm) to be the numerical limits for a single session of GKS, if the peripheral dose is 20 Gy with the GammaPlan. Adverse early radiation effects such as acute brain swelling were not observed in our series. Research groups of Yamamoto and Yang, using higher radiation doses than allowed by the criteria employed herein, reported the safety of GKS for numerous brain metastases [16, 17]. From the viewpoint of our large series and routine WBRT use, a mean whole brain radiation dose of 3 Gy seems to be quite safe, if lesions are diffusely scattered in the brain. Furthermore, this study found patients with carcinomatous meningitis to have significantly poorer NS and QS. In conclusion, our present criteria indicating GKS alone to be suitable for treating metastatic brain tumours are 1) no surgically inaccessible large (>30 mm) tumours, 2) 10 or fewer lesions, 3) a maximum of 3 tumours with a diameter ≥25 mm, and 4) no findings of carcinomatous meningitis on MRI. NS and QS for one year of patients with these criteria were 91.5% and 81.6%, respectively.

It has become widely accepted, since the advent of CT scanning, that even patients with only a single metastatic lesion have microscopic metastases [8]. Modern high-quality MRI can detect metastatic tumours only a few millimeters in diameter. The survival period may be too short for invisible metastases or true new lesions to be identified on follow-up MRI or to cause neurological symptoms and signs. Chemotherapy may, of course, play an additional role in controlling microscopic lesions. Our treatment policy for metastatic brain tumours is that verifiable local control is the first priority, while treating invisible metastases is the second. Indeed, almost 60% of patients in our series did not require salvage treatment. Upfront WBRT need not be introduced and appropriate salvage treatment, taking the patient's condition into consideration, may be warranted, if new lesions are detected. The current study demonstrates that a local GKS treatment protocol without upfront WBRT can provide highly satisfactory results in selected patients with close observation and appropriate salvage treatment.

Conclusions

From the viewpoints of NS and QS, GKS without upfront WBRT for brain metastases from various primary tumours provides satisfactory palliation considering the patients' short life expectancies. Brain metastases could be managed according to our local treatment protocol by GKS alone without upfront WBRT, if the following 4 criteria were satisfied 1) no surgically inaccessible large (>30 mm) tumours, 2) 10 or fewer lesions, 3) a maximum of 3 tumours with a diameter of ≥25 mm, and 4) no findings of carcinomatous meningitis on MRI. However, careful follow-up MRI and appropriate salvage treatment are essential to preventing neurological death and maintaining favorable ADL.

References

1. Asai A, Matsutani M, Kohno T, Nakamura O, Tanaka H, Fujimaki T, Funada N, Matsuda T, Nagata K, Takakura K (1989) Subacute brain atrophy after irradiation therapy for malignant brain tumor. Cancer 63: 1962–1974
2. Buatti JM, Friedman WA, Bova FJ, Mendenhall WM (1995) Treatment selection factors for stereotactic radiosurgery of intracranial metastases. Int J Radiat Oncol Biol Phys 32(4): 1161–1166
3. Cho KH, Hall WA, Gerbi BJ, Higgins PD, Bohen M, Clark HB (1998) Patient selection criteria for the treatment of brain metastases with stereotactic radiosurgery. J Neuro Oncol 40(1): 73–86
4. DeAngelis LM, Delattre JY, Posner JB (1989) Radiation-induced dementia in patients cured of brain metastases. Neurology 39: 789–796
5. Flickinger JC, Kondziolka D, Lunsford LD, Coffey RJ, Goodman ML, Shaw EG, Hudgins WR, Weiner R, Harsh GR 4th, Sneed PK (1994) A multi-institutional experience with stereotactic radiosurgery for solitary brain metastasis. Int J Radiat Oncol Biol Phys 28(4): 797–802
6. Hasegawa T, Kondziolka D, Flickinger JC, Germanwala A, Lunsford LD (2003) Brain metastases treated with radiosurgery alone: an alternative to whole brain radiotherapy? Neurosurgery 52: 1318–1326
7. Kondziolka D, Patel A, Lunsford LD, Kassam A, Flickinger JC (1999) Stereotactic radiosurgery plus whole brain radiotherapy versus radiotherapy alone for patients with multiple brain metastases. Int J Radiat Oncol Biol Phys 45: 427–737
8. Patchell RA, Tibbs PA, Walsh JW, Dempsey RJ, Maruyama Y, Kryscio RJ, Markesbery WR, MacDonald TS, Young B (1990) A randomized trial of surgery in the treatment of single metastases to the brain. N Engl J Med 322: 494–500
9. Patchell RA, Regine WF (2003) The rationale for adjuvant whole brain radiation therapy with radiosurgery in the treatment of single brain metastases. Technol Cancer Res Treat 2(2): 111–116
10. Serizawa T, Iuchi T, Ono J, Saeki N, Osato K, Odaki M, Ushikubo O, Hirai S, Sato M, Matsuda S (2000) Gamma knife treatment for multiple metastatic brain tumors compared with whole-brain radiation therapy. J Neurosurg [Suppl] 3(93): 32–36
11. Serizawa T, Ono J, Iuchi T, Matsuda S, Sato M, Odaki M, Hirai S, Osato K, Saeki N, Yamaura A (2002) Gamma knife radiosurgery for metastatic brain tumors from lung cancer. Comparison between small cell cancer and non-small cell cancer. J Neurosurg [Suppl] 5(97): 484–488
12. Serizawa T, Saeki N, Higuchi Y, Ono J, Matsuda S, Sato M, Yanagisawa M, Iuchi T, Nagano O, Yamaura A, Ono J, Odaki M, Hirai S, Sato M, Matsuda S, Yanagisawa M, Maru S, Iwase T, Sato M (2005) Diagnostic value of thallium-201 chloride single-photon emission computed tomography in differentiating tumor recurrence from radiation injury after gamma knife surgery for metastatic brain tumors. J Neurosurg [Suppl] 2(102): 266–271
13. Shimonova G, Liscak R, Novotny J Jr, Novotony J (2000) Solitary brain metastases treated with the Leksell gamma knife: prognostic factors for patients. Radiother Oncol 57(2): 207–213
14. Sneed PK, Lamborn KR, Forstner JM, McDermott MW, Chang S, Park E, Gutin PH, Phillips TL, Wara WM, Larson DA (1999) Radiosurgery for brain metastases: is whole brain radiotherapy necessary? Int J Radiat Oncol Biol Phys 43(3): 549–558
15. Sneed PK, Suh JH, Goetsch SJ, Sanghavi SN, Chappell R, Buatti JM, Regine WF, Weltman E, King VJ, Breneman JC, Sperduto PW, Mehta MP (2002) A multi-institutional review of radiosurgery alone vs. radiosurgery with whole brain radiotherapy as the initial management of brain metastases. Int J Radiat Oncol Biol Phys 53(3): 519–526
16. Yang CC, Ting J, Wu X, Markoe A (1998) Dose volume histogram analysis of the gamma knife radiosurgery treating twenty-five metastatic intracranial tumors. Stereotactic Funct Neurosurg 70: 41–49
17. Yamamoto M, Ide M, Nishio S, Urakawa Y (2002) Gamma knife radiosurgery for numerous brain metastases: Is this a safe treatment? Int J Radiat Oncol Biol Phys 53(5): 1279–1283

Comment

This is an interesting and potentially important paper. As some other authorities have done before them, the authors have challenged the traditional wisdom of limiting gamma knife surgery to the maximum of 3 lesions. Inclusion criteria for this study were patients with a maximum of 3 tumours with a diameter $\geq$25 mm, no cerebral dissemination ($\leq$25 micrometastases) and no surgically inaccessible large (>30 mm) tumours. This reviewer from the United Kingdom read with great interest, that in several of their patients salvage treatment was carried out, in nine cases five times or more. This raises an interesting question about healthcare funding.

They have, very usefully, extended the outcome measures from overall survival to include death from neurological causes, qualitative survival, new lesion free survival, progression free survival etc.

They have shown that there is no significant reduction in outcome up to 10 lesions when a wide variety of outcome measures are considered. They have truly tested the technique, by going up to 77 lesions in one case.

The observations made are sound if not particularly surprising. Active extracranial disease, poor pretreatment Karnofsky score and carcinomatous meningitis were confirmed to be significant factors influencing outcome. At this stage of our knowledge their recommendations: no surgically inaccessible large tumours, 10 or fewer lesions, a maximum of 3 tumours with a diameter of $\geq$25 mm, and no carcinomatous meningitis, appear sensible.

Andras Kemeny
Sheffield

Correspondence: Toru Serizawa, Department of Neurosurgery, Chiba Cardiovascular Center, 575 Tsurumai, Ichihara, Chiba, 2900512 Japan. e-mail: QWT03231@nifty.ne.jp

J Neurosurg (Suppl) 102:266–271, 2005

Diagnostic value of thallium-201 chloride single-photon emission computerized tomography in differentiating tumor recurrence from radiation injury after gamma knife surgery for metastatic brain tumors

TORU SERIZAWA, M.D., PH.D., NAOKATSU SAEKI, M.D., PH.D., YOSHINORI HIGUCHI, M.D. PH.D., JUNICHI ONO, M.D., PH.D., SHINJI MATSUDA, M.D., PH.D., MAKOTO SATO, R.T., MASAMICHI YANAGISAWA, R.T., TOSHIHIKO IUCHI, M.D., PH.D., OSAMU NAGANO, M.D., AND AKIRA YAMAURA, M.D., PH.D.

Departments of Neurosurgery, Neurology, and Radiology, Chiba Cardiovascular Center, Ichihara, Japan; and Division of Neurological Surgery, Chiba Cancer Center; and Department of Neurological Surgery, Graduate School of Medicine, Chiba University, Chiba, Japan

Object. The authors assessed the diagnostic value of ^{201}Tl Cl single-photon emission computerized tomography (SPECT), performed after gamma knife surgery (GKS) for metastatic brain tumors in differentiating tumor recurrence from radiation injury.

Methods. Of 6503 metastatic brain tumors treated with GKS, ^{201}Tl SPECT was required in 72 to differentiate between tumor recurrence and radiation injury. When the Tl index was greater than 5, the lesion was diagnosed as a tumor recurrence. When the index was < 3.0 it was called radiation injury. In cases with a Tl index between 3 and 5, ^{201}Tl SPECT was repeated once per month until the Tl index was greater than 5 or less than 3. If the Tl index fluctuated between 3 and 5 for 2 months, the lesion was diagnosed as radiation injury. The final diagnosis was based on histological examination or clinical course.

The sensitivity of the method was 91%; thus ^{201}Tl SPECT is effective for differentiating between tumor recurrence and radiation injury in metastatic brain tumors treated with GKS. Caution is necessary, however, for the following reasons: 1) simple interinstitutional comparisons of Tl indices are not possible because measurement methods are institute specific; 2) steroid administration decreases the Tl index to a variable degree; and 3) a severe radiation injury lesion, as is often seen after repeated GKS or very high dose GKS, may have a Tl index greater than 5.

Conclusions. Used with critical insight ^{201}Tl Cl SPECT can be useful in distinguishing between tumor regrowth and radiation necrosis in patients with cerebral metastases.

KEY WORDS • **gamma knife surgery** • **metastatic brain tumor** • **radiation injury** • **tumor recurrence** • **thallium-201** • **single-photon emission computerized tomography**

EXCELLENT tumor control has been reported using GKS for metastatic brain tumors that result from various systemic malignancies; however, tumor regrowth with surrounding edema can occur after GKS.[8,10] In this situation, differentiating between tumor recurrence and radiation injury may be difficult using only MR imaging. The purpose of this prospective study was to determine the differential diagnostic value of ^{201}Tl Cl SPECT after GKS for metastatic brain tumors.

Clinical Material and Methods

Among 701 patients with 6503 metastatic brain tumors 1404 were treated with GKS between 1998 and 2003. Of these 72 lesions in 70 patients in whom regrowth was demonstrated on follow-up MR imaging were studied with

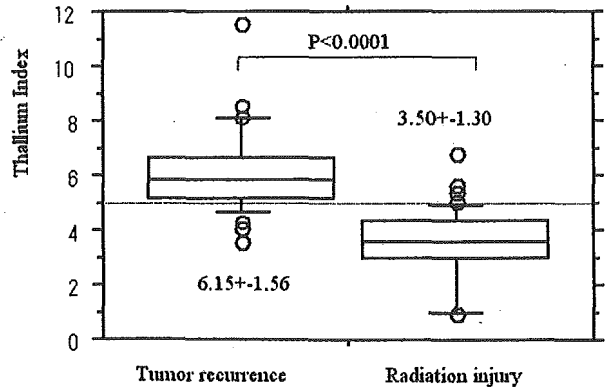

FIG. 1. Graph showing the distribution of Tl indices.

Abbreviations used in this paper: GKS = gamma knife surgery; MR = magnetic resonance; SPECT = single-photon emission computerized tomography.

TABLE 1

*Treatment summary of 72 lesions**

Variable	Min	Max	Mean	SD	Median
tumor vol (cm^3)	0.25	16.0	5.73	4.44	4.70
peripheral (%)	38.1	91.6	53.6	10.7	49.9
peripheral dose (Gy)	14.0	30.0	20.4	2.7	20.0
max dose (Gy)	24.8	59.8	28.9	6.9	40.1
no. of isocenters	1	24	8.2	5.8	6.5

* SD = standard deviation.

^{201}Tl SPECT and analyzed for this study. The mean patient age was 63.8 years (range 46–86 years). There were 37 men and 33 women. The primary cancer was from the lung in 57 (79.2%), gastrointestinal tract in 10 (13.9%), urinary tract in two (2.8%), breast in one (1.4%), and other in two (2.8%). The early Tl index was quantified using a triple-head gamma camera equipped with low-energy high-resolution fan beam collimators (GCA9300A/UI; Toshiba, Tokyo, Japan). The data were acquired in a 128 × 128 matrix over a 120° rotation at angular intervals of 4°. The energy was set at 75 keV for the main window and at 7% for the subwindow. Data were collected 20 minutes after intravenous administration of 111 MBq ^{201}Tl. Scatter correction was performed by the triple-energy window method, but absorption correction was not used. The SPECT images were gathered after filtered-back projection with a Butterworth filter (cut-off frequency 0.34 cycles/cm). The region of interest was automatically drawn with a lower cut-off for the lesion at 80%, to minimize errors between radiation technicians. The control region, approximately 100 pixels, was the contralateral or distant normal brain.

When the Tl index was greater than 5, the lesion was diagnosed as tumor recurrence. If the index was less than 3 the lesion was diagnosed as radiation injury. In cases in which the Tl index was between 3 and 5, ^{201}Tl SPECT was repeated once per month until the Tl index was either greater than 5 or less than 3. If the Tl index fluctuated between 3 and 5 for 2 months, the lesion was diagnosed as radiation injury. The final diagnosis was based on histological examination or clinical course. In patients whose lesions did not undergo histological examination, radiation injury was diagnosed when the enhanced lesion did not increase in size on subsequent MR imaging for 3 months or more. A paired Student t-test was used to compare the Tl indices of tumor recurrence with those of radiation injury. A probability value less than 0.05 was considered statistically significant.

Results

The treatment data are summarized in Table 1. The mean tumor volume was 5.8 cm^3, and the mean radiation dose at the periphery was 20.5 Gy. The mean number of isocenters was 8.4. The mean interval from GKS to the first radioisotope diagnosis was 7.3 months (range 1.2–44.6 months). The equivalent mean interval to the last radioisotope diagnosis was 8.7 months (range 2.1–44.6 months). Thirty-one

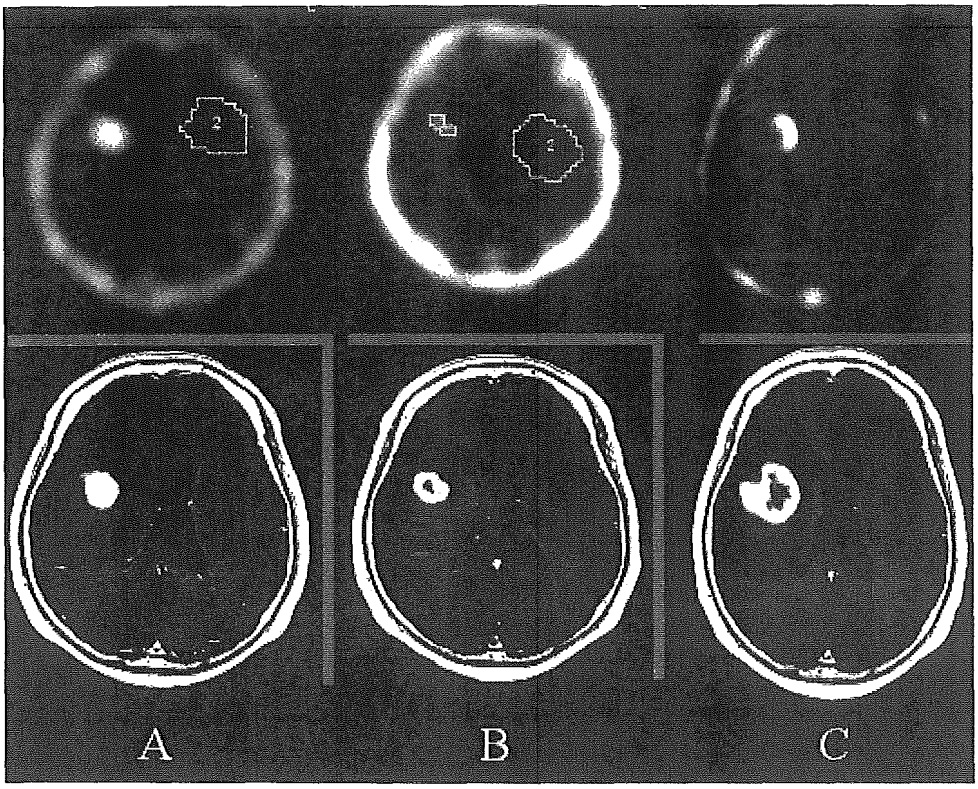

FIG. 2. Serial enhanced MR and ^{201}Tl SPECT studies obtained in the patient in Case 1. A: Pre-GKS: a right frontal metastatic lesion from colon cancer. The Tl accumulation was intense (Tl index 11.43). B: Two months later: the tumor shows shrinkage and the Tl index has decreased to 2.75. C: Seven months later the tumor has increased in size and the Tl index has risen to 5.8. The radioisotope diagnosis was tumor recurrence. The tumor was resected.

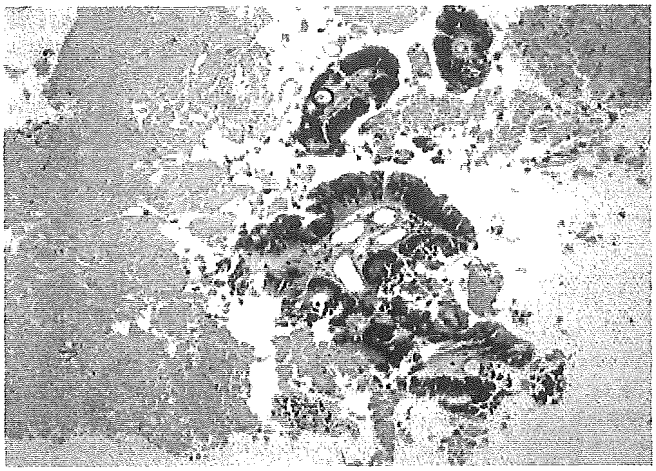

FIG. 3. Photomicrograph obtained in Case 1. Histopathological examination confirmed viable tumor cells. H & E.

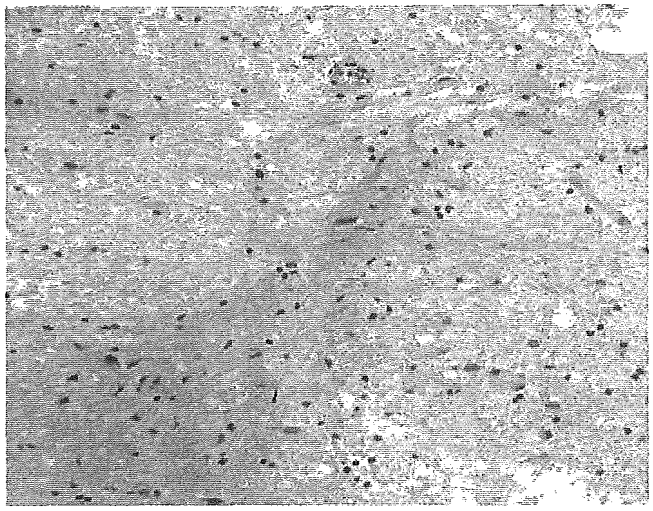

FIG. 5. Photomicrograph obtained in Case 2. This specimen was obtained by MR-guided stereotactic biopsy and shows no viable tumor cells

lesions (43.1%) were diagnosed based only on the first Tl index measurement, and 41 (56.9%) required serial Tl measurements. Distributions of the Tl index are shown in Fig. 1. The mean Tl indices of tumor recurrence and radiation injury were 6.15 and 3.5, respectively, a statistically significant difference ($p < 0.0001$). The final diagnosis was tumor recurrence in 30 and radiation injury in 42. Ten lesions (14.1%) were histopathologically examined. There were three false-positives and four false-negative results. For 65 lesions, the radioisotope and final diagnoses were compatible (accuracy 90.3%). Sensitivity was 90% and specificity was 90.5%.

Case Presentation

Case 1. Tumor Recurrence. This 62-year-old woman had a single 25-mm metastatic lesion in the frontal lobe from colon cancer (Fig. 2A). The pre-GKS Tl index was 11.43. The lesion was treated by GKS with 26 Gy to the 52% isodose line. Gadolinium-enhanced MR imaging obtained 2 months later revealed tumor shrinkage (Fig. 2B) and the Tl index had decreased to 2.75. Seven months later, however, MR imaging demonstrated tumor regrowth (Fig. 2C) and the Tl index had increased to 5.8. The radioisotope diagnosis was tumor recurrence. The tumor was surgically removed, and histopathological examination revealed viable tumor cells (Fig. 3).

Case 2. Radiation Injury. This 72-year-old man had multiple brain metastases from lung adenocarcinoma. A lesion in the caudate nucleus was irradiated with 22 Gy to the 50% isodose line (Fig. 4A). The pre-GKS Tl index was 4.63. Two months later MR imaging revealed marked tumor shrinkage (Fig. 4B), and there was no abnormal Tl accumulation. Six months later, MR imaging demonstrated tumor regrowth (Fig. 4C) and the Tl index was low but not

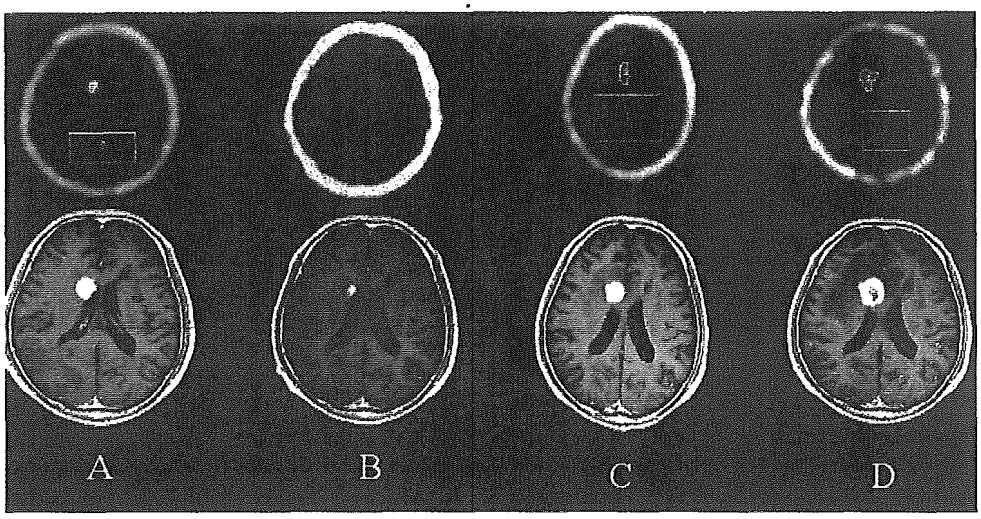

FIG. 4. Serial enhanced MR image and ^{201}Tl SPECT studies obtained in the patient in Case 2. A: Pre-GKS: a metastatic lesion in the right caudate from lung adenocarcinoma. The pre-GKS Tl index was 4.63. B: Two months later the tumor shows marked shrinkage. There is no abnormal Tl accumulation. C: Six months later MR imaging demonstrated tumor regrowth, but the Tl index remains low (3.08), necessitating serial measurements. D: Eight months later the area of enhancement has again increased in size. The Tl index remains low (3.43). The radioisotope diagnosis was radiation injury.

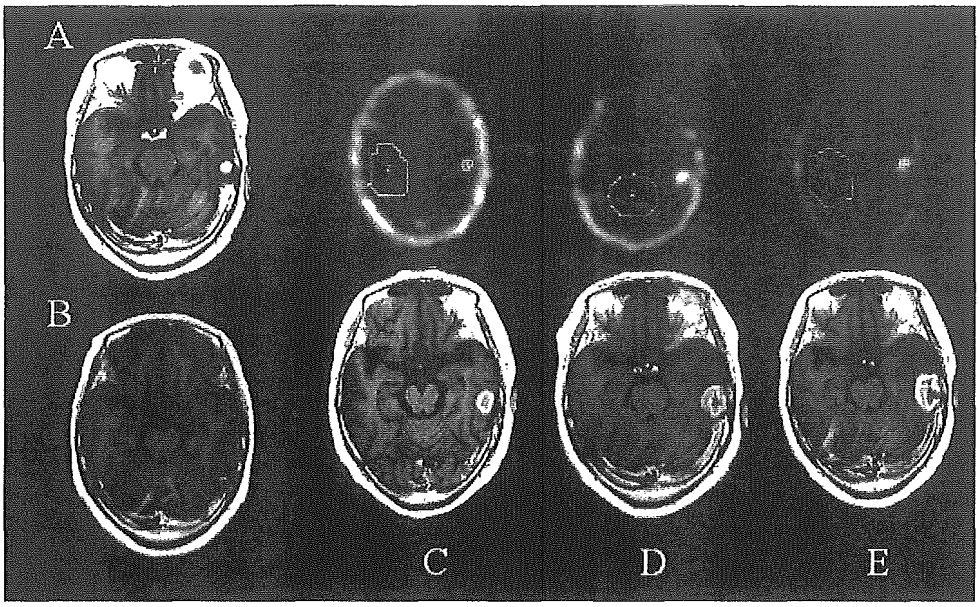

FIG. 6. Serial enhanced MR and ^{201}Tl SPECT studies obtained in the patient in Case 3. A: A small left temporal metastatic tumor from breast cancer was treated by GKS. B: Two months later, the tumor has completely disappeared. C: Six months later, tumor regrowth is apparent. Thallium-201 accumulation is low (3.10). The radioisotope diagnosis was radiation injury at this initial study. D: Eight months later the tumor continued to grow. Abnormally high Tl accumulation in the posterior part of the enhanced area (Tl index 5.18) is consistent with a radioisotope diagnosis of tumor recurrence. The tumor was treated again with GKS, using a peripheral dose of 20 Gy. E: Ten months later, the tumor continued to grow. Thallium-201 accumulated in the anterior portion of the area showing enhancement (Tl index 5.12). The patient exhibited sensory aphasia. The tumor was surgically removed 3 months after repeated GKS.

low enough to be definitive, which necessitated serial measurements. Eight months later MR imaging demonstrated a further increase in size, and the index was 3.43. The radioisotope diagnosis was radiation injury. A specimen obtained by MR imaging–guided stereotactic biopsy revealed no viable tumor cells (Fig. 5).

Case 3. Radiation Injury. This 58-year-old woman had multiple brain metastases from breast cancer. A small peripheral lesion in the temporal lobe was irradiated with 20 Gy to the 80% isodose line (Fig. 6A). Two months later MR imaging revealed complete remission (Fig. 6B). Eight months later MR imaging revealed tumor growth (Fig. 6C). There was an abnormally high Tl accumulation in the posterior part of a mass, which showed enhancement, and the Tl index was 5.18, indicating tumor recurrence. The tumor was irradiated again with a peripheral dose of 20 Gy to the 55% isodose line. Further tumor growth was seen on MR imaging 10 months later, that is 2 months after the second GKS. There was Tl accumulation in the anterior part of the area showing enhancement. The Tl index was still high at 5.12 (Fig. 6D). The patient exhibited sensory aphasia despite steroid administration. The tumor was surgically removed 3 months after the second GKS. The pathological examination confirmed pure radiation injury as shown in Fig. 7.

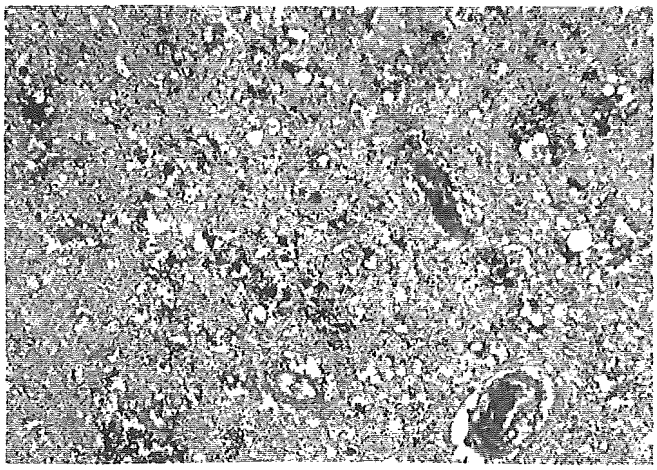

FIG. 7. Photomicrograph obtained in Case 3. The pathological examination confirmed radiation injury. H & E.

Discussion

Over the last two decades extensive research focusing on various methods, such as positron emission tomography scanning using ^{18}F-fluorodeoxyglucose or L-methyl-^{11}C-methionine, SPECT using ^{201}Tl and ^{99m}-Tc-hexakis-2-methoxy-isobutylisonitrile, and MR spectroscopy, has provided invaluable information facilitating the differential diagnosis of tumor recurrence from radiation injury.[1–3,6,7,11] Thallium-201, already used as a cardiomuscle tracer, was discovered to accumulate in various brain tumors, and reports on differential diagnosis of brain tumors and assessment after radiotherapy have been published.[4,9] We have endeavored to differentiate regrowth of lesions after GKS by using this classic tracer. We introduced scatter correction with the triple-energy window method, a more sensitive detection technique, which has a higher Tl index than conventional methods. This allowed us to differentiate tumor

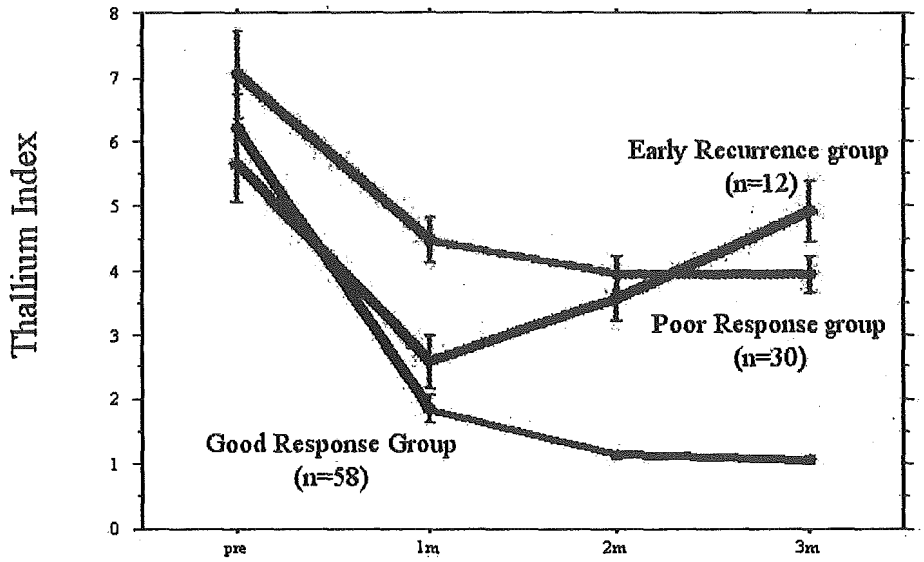

FIG. 8. Monthly serial Tl indices after GKS for 100 metastatic lesions were obtained in a pilot study. There were three patterns of Tl index change. 1: Good response type showing a continuous decrease to 1, within 2 or 3 months after GKS (blue, 58 lesions). 2) Early recurrence type demonstrating a transient decrease at 1 month but an increase to 5, within 3 months after GKS (red, 12 lesions). 3) Poor response type showing a transient decrease at 1 month and a fluctuation between 3 and 5, at 2 to 3 months after GKS (green, 30 lesions).

recurrence from radiation injury with higher sensitivity than would have been possible with conventional measurement methods. Furthermore, MR imaging following SPECT studies is performed within 1 hour after simultaneous intravenous injection of ^{201}Tl and Gd during serial measurements. These innovations make it possible to examine patients with tumor regrowth easily and quickly.

In a lesion that starts to grow again after GKS, tumor recurrence and radiation injury are not mutually exclusive because both components may be present. In this situation, it is crucial to ascertain when the recurrent components begin to grow and require retreatment. We identify a gray zone in which the Tl index is between 3 and 5 to determine whether a mixed lesion represents true recurrence. In cases with a Tl index in this gray zone, ^{201}Tl SPECT studies are repeated once per month until the Tl index exceeds 5 or is less than 3. A frequency of observation of every other month is considered adequate for serial measurements. With radiation injury, the Tl index usually fluctuates, whereas in a recurrent tumor it usually increases monthly. This pattern provides important information facilitating differentiation.

The cut-off value we used was derived from a pilot study of monthly serial Tl measurements after GKS in 100 metastatic lesions (Fig. 7). That study demonstrated three patterns of Tl index change, which were classified as follows. 1) Good response: showing a continuous decrease to 1, within 2 to 3 months after GKS (58 lesions). 2) Early recurrence: demonstrating a transient decrease at 1 month and an increase to 5 at 3 months (12 lesions). 3) Poor response: showing a transient decrease at 1 month and fluctuation between 3 and 5 at 2 to 3 months after GKS (30 lesions).

Setting the cut-off value at 5 was based on these results, as we previously reported.[9] The "poor response" type represents tumor recurrence followed later by radiation injury. This is why we consider values between 3 and 5 to represent a gray zone.

Thallium-201 chloride SPECT scanning does have limitations. The first is that a simple interinstitutional comparison of Tl indices is not possible because measurement methods are institute specific. Thus, serial measurements must be performed under the same conditions at the same institute. Second, steroid use decreases the Tl index to a variable degree, as reported by Namba, et al.[5] This reduction may be attributed to steroid administration, which decreases the uptake of ^{201}Tl into viable tumor cells and the inflammatory portion of a radiation injury lesion. This phenomenon must be kept in mind, especially with serial Tl measurements. Finally, highly inflammatory lesions associated with radiation injury, such as occurs after repeated GKS or with high-dose GKS, may produce a Tl index greater than 5, as in our Case 3.

Conclusions

Thallium-201 chloride SPECT scanning can be effective for differentiating tumor recurrence from radiation injury in metastatic brain tumors treated with GKS. The technique is appropriate as long as the technical limitations of the method are kept in mind.

References

1. Belohlavek O, Simonova G, Kantorova I, et al: Brain metastases after stereotactic radiosurgery using the Leksell gamma knife: can FDG PET help to differentiate radionecrosis from tumor progression? **Eur J Nucl Med Mol Imaging 30:**96–100, 2003
2. Chao ST, Suh JH, Raja S, et al: The sensitivity and specificity of FDG PET in distinguishing recurrent brain tumor from radionecrosis in patients treated with stereotactic radiosurgery. **Int J Cancer 96:**191–197, 2001
3. Hinoda J, Yano H, Ando H, et al: Radiological response and histological changes in malignant astrocytic tumors after stereotactic radiosurgery. **Brain Tumor Pathol 19:**83–92, 2002
4. Kosuda S, Fujii H, Aoki S, et al: Reassessment of quantitative thal-

lium-201 brain SPECT for miscellaneous brain tumors. **Ann Nucl Med 7:**257–263, 1993
5. Namba H, Togawa T, Yui N, et al: The effect of steroid on thallium-201 uptake by malignant gliomas. **Eur J Nucl Med 23:** 991–992, 1996
6. Rock JP, Hearshen D, Scarpace L, et al: Correlations between magnetic resonance spectroscopy and image-guided histopathology, with special attention to radiation necrosis. **Neurosurgery 51:** 912–919, 2002
7. Schlemmer HP, Bachert P, Henze M, et al: Differentiation of radiation necrosis from tumor progression using proton magnetic resonance spectroscopy. **Neuroradiology 44:**216–222, 2002
8. Serizawa T, Ono J, Iuchi T, et al: Gamma knife treatment for multiple metastatic brain tumors compared with whole-brain radiation therapy. **J Neurosurg (Suppl 3) 93:**32–36, 2000
9. Serizawa T, Ono J, Odaki M, et al: Differentiation between tumor recurrence and radiation injury after gamma knife radiosurgery for metastatic brain tumors: value of serial Thallium-201 Chloride SPECT. **Jpn J Neurosurg 10:**726–732, 2001 (In Japanese with English abstract)
10. Serizawa T, Ono J, Iuchi T, et al: Gamma knife radiosurgery for metastatic brain tumors from lung cancer—Comparison between small cell cancer and non-small cell cancer. **J Neurosurg (Suppl 5) 97:**484–488, 2002
11. Tsuyuguchi N, Sunada I, Iwai Y, et al: Methionine positron emission tomography of recurrent metastatic brain tumor and radiation necrosis after stereotactic radiosurgery: is a differential diagnosis possible? **J Neurosurg 98:**1056–1064, 2003

Address reprint requests to: Toru Serizawa, M.D., Ph.D., Department of Neurosurgery, Chiba Cardiovascular Center, 575 Tsurumai, Ichihara, Chiba, 2900512, Japan. email: QWT03231@nifty.ne.jp.

Recombinant Sendai Virus Vector Induces Complete Remission of Established Brain Tumors through Efficient *Interleukin-2* Gene Transfer in Vaccinated Rats

Yasuo Iwadate,[1] Makoto Inoue,[4] Takashi Saegusa,[1] Yumiko Tokusumi,[4] Hiroaki Kinoh,[4] Mamoru Hasegawa,[4] Masatoshi Tagawa,[3] Akira Yamaura,[1] and Hideaki Shimada[2]

Abstract

Purpose: Sendai virus (SeV), a murine parainfluenza virus type I, replicates independent of cellular genome and directs high-level gene expressions when used as a viral vector. We constructed a nontransmissible recombinant SeV vector by deleting the *matrix (M)* and *fusion (F)* genes from its genome (SeV/ΔMΔF) to enhance its safety. We also estimated the therapeutic efficacy of the novel vector system against a rat glioblastoma model.

Experimental Design: We administered the recombinant SeV vector carrying the *lacZ* gene or the *human interleukin-2* (*hIL-2*) gene into established 9L brain tumors *in vivo* simultaneous with peripheral vaccination using irradiated 9L cells. Sequential monitoring with magnetic resonance imaging was used to evaluate the therapeutic efficacy.

Results: We found extensive transduction of the *lacZ* gene into the brain tumors and confirmed sufficient amounts of interleukin 2 (IL-2) production by hIL2-SeV/ΔMΔF both *in vitro* and *in vivo*. The magnetic resonance imaging study showed that the intracerebral injection of hIL2-SeV/ΔMΔF brought about significant reduction of the tumor growth, including complete elimination of the established brain tumors. The ^{51}Cr release assay showed that significant amounts of 9L-specific cytotoxic T cells were induced by the peripheral vaccination. Immunohistochemical analysis revealed that $CD4^+$ T cells and $CD8^+$ T cells were abundantly infiltrated in the target tumors.

Conclusion: The present results show that the recombinant nontransmissible SeV vector provides efficient *in vivo* gene transfer that induces significant regression of the established brain tumors and suggest that it will be a safe and useful viral vector for the clinical practice of glioma gene therapy.

Glioblastoma is the most common malignant brain tumor. It is considered incurable despite multimodal approaches of therapy, including surgery, radiotherapy, and chemotherapy (1). The therapeutic application of the gene transfer technique has been expected as a new therapeutic option for glioblastoma (2). The efficacy, however, has been limited by low levels of transgene transduction and poor distribution of the target molecules throughout the tumor tissues (3). The successful gene therapy in clinical practice will depend on the development of novel vector systems capable of wide distribution and efficient transduction of the target genes into the tumor cells.

Recent advances to manipulate the genome of negative-strand RNA viruses have led to the development of a new class of viral vectors for gene transfer approaches (4). Sendai virus (SeV) is a murine parainfluenza virus type I belonging to the family Paramyxoviridae and is a single-stranded RNA virus. The genome of SeV is a linear and nonsegmented negative-strand RNA of ~15.4 kb. It contains six major genes that are arranged in tandem on its genome; it is tightly encapsidated with the nucleoprotein (NP) and is further complexed to phosphoprotein (P) and large protein (L; the catalytic subunit of the polymerase). This viral ribonucleoprotein complex constitutes the internal core structure of the virion. The viral envelope contains two spike proteins, hemagglutinin-neuraminidase (HN) and fusion (F), which mediate the attachment of virions and the penetration of ribonucleoproteins into infected cells, respectively. Matrix (M) protein functions in virus assembly and budding.

For the use of gene therapy vectors, the promising characteristics of SeV are as follows: (*a*) an exclusively cytoplasmic replication cycle without any risk of integration into the genomic DNA, (*b*) transduction efficacy that is not dependent on the cell cycle of target cells, (*c*) no homologous recombination between

Authors' Affiliations: Departments of [1]Neurological Surgery and [2]Academic Surgery, Graduate School of Medicine, Chiba University; [3]Division of Pathology, Chiba Cancer Center Research Institute, Chiba, Japan; and [4]DNAVEC Research, Inc., Tsukuba, Ibaraki, Japan

Received 7/28/04; revised 12/1/04; accepted 12/22/04.

Grant support: Grant-in-aid for scientific research from Japan Society for the Promotion of Science and a grant-in-aid for scientific research on priority areas from the Minister of Education, Culture, Sports, Science, and Technology of Japan.

The costs of publication of this article were defrayed in part by the payment of page charges. This article must therefore be hereby marked *advertisement* in accordance with 18 U.S.C. Section 1734 solely to indicate this fact.

Requests for reprints: Yasuo Iwadate, Department of Neurological Surgery, Chiba University Graduate School of Medicine, 1-8-1 Inohana, Chuo-ku, 260-8670 Chiba, Japan. Phone: 81-43-226-2158; Fax: 81-43-226-2159; E-mail: iwadatey@faculty.chiba-u.jp.

different SeV genomes or to wild-type virus, (*d*) the remarkably brief contact time that is necessary for cellular uptake, (*e*) a high and adjustable expression of virally encoded genes in a broad range of host cells, and (*f*) the lack of association with any disease process in humans (4). Indeed, the SeV vector has been shown to produce 2 to 3 logs higher transfection efficiency than the adenoviral vectors or lipofection (5, 6), and high gene expressions have been noticed in a broad range of tissues, including the airway epithelial cells, vasculature tissues, skeletal muscle, activated T cells, stem cells, and neural tissues (5–12). In addition to these biological features of the SeV vector, we have constructed a nontransmissible recombinant SeV vector by deleting the M and F genes from its genome to enhance its safety (13–15).

We previously verified the efficacy of the intracerebral (i.c.) transplantation of interleukin 2 (IL-2)–producing cells in the rat brain tumor model (16, 17). For clinical application of the cytokine gene therapy strategy, however, the cell-mediated therapy needs a large amount of cytokine-producing cells to cover the whole tumor areas in the human brain. The SeV vector–mediated strategy would be superior in the wide distribution of the transgene products achieved by a small amount of viral solution, and it is expected to be especially suitable for delivery of the secreted proteins, such as cytokines. In the present study, we examined the therapeutic potentials of the nontransmissible recombinant SeV vector carrying *human IL-2* gene in a cytokine gene therapy against brain tumors.

Materials and Methods

Cells and animals. Rat 9L gliosarcoma, C6 glioma, and rhesus monkey LLC-MK_2 kidney cell lines were maintained in DMEM supplemented with 10% FCS in a humidified atmosphere of 5% CO_2. Male Fisher 344 rats, weighing between 200 and 240 g (7-8 weeks old) were used as indicated in the experiments. These animals were maintained in a specific pathogen-free environment in accordance with the Laboratory Animal Resources Commission Standards.

Recombinant Sendai virus vector. Genome order of the SeV full length genome used was as follows: the leader (ld) at the 3′-end followed by viral genes, *nucleocapsid (NP), phospho (P), matrix (M), fusion (F), hemagglutinin-neuraminidase (HN),* and *large proteins (L)*. Finally, a small trailer (tr) sequence was placed at the 5′-end (Fig. 1). We utilized both the *M* and *F* genes–deleted SeV vector (SeV ΔMΔF) in the experiment. F protein is essential for viral infection and M protein functions in virus assembly and budding (13, 14). Therefore, SeV/ΔMΔF is nontransmissible with loss of particle formation from infected cells (15). SeV/ΔMΔF carrying *human IL-2* gene (hIL2-SeV/ΔMΔF) and *lacZ* gene (lacZ-SeV/ΔMΔF) were constructed as previously described (13). In brief, human IL-2 (accession no. U25676) cDNA was amplified with a pair of *Not*I-tagged primers that contained SeV-specific transcriptional regulatory signal sequences, 5′-ACTTGCGGCCGCGTTTAAACGGCGCGCCATGTACAGGATG-CAACTCCTGTC-3′ and 5′-ATCCGCGGCCGCGATGAACTTTCACCC-TAAGTTTTTCTTACTACGGATTTAAATGGCGCGCCA-3′. The amplified fragment was introduced into the *Not*I site of the parental pSeV18+/ΔMΔF. Thus, the cDNA of hIL2-SeV/ΔMΔF (phIL2-SeV/ΔMΔF) was constructed. The cDNA of lacZ-SeV/ΔMΔF (placZ-SeV/ΔMΔF) was constructed in similar manner using the amplified fragment of lacZ (18). phIL2-SeV/ΔMΔF and placZ-SeV/ΔMΔF were transfected into LLC-MK_2 cells after infection of the cells with vaccinia virus vTF7-3 (19), which expresses T7 polymerase. The T7-driven recombinant hIL2-SeV/ΔMΔF and lacZ-SeV/ΔMΔF RNA genomes were encapsulated by N, P, and L proteins, which were derived from their respective cotransfected plasmids. The recovered SeV vectors were propagated using both M and F protein–expressing packaging cell lines (15). The virus titers were determined using infectivity and were expressed in cell infectious units. The SeV vectors were stored at −80°C until use.

Kinetic analysis of interleukin-2 production. LLC-MK_2 cells (10^6) grown in six-well plates were infected at a multiplicity of infection of 10 for 1 hour with hIL2-SeV/ΔMΔF and incubated in serum-free MEM at 37°C. The culture supernatants were collected every 24 hours, with immediate addition of MEM to the remaining cells. IL-2 protein in the supernatant was quantified by ELISA using the human IL-2 ELISA kit (Biosource International, Inc., Camarillo, CA).

Brain tumor model and treatment. The animals were anesthetized and placed in a stereotaxic apparatus. A burr hole was made at 4 mm posterior to bregma and 3 mm right to midline. A 25-gauge needle was inserted to the point of 3 mm ventral from dura where 1×10^5 syngeneic 9L tumor cells in 10 μL medium were slowly injected. Treatment was started 3 days (day 3) after i.c. inoculation of 9L tumor cells (day 0). The animals received i.c. administration of hIL2-SeV/ΔMΔF or lacZ-SeV/ΔMΔF and/or s.c. vaccination with irradiated wild-type 9L tumor cells. For i.c. administration, 1×10^7 cell infectious units of SeV vector in 10 μL PBS were used in the same stereotactic coordinates. For s.c. vaccination, wild-type 9L cells were irradiated at 30 Gy and 1×10^6 cells in 100 μL medium were injected into the lower abdominal quadrant (16, 17). The animal experimentation was reviewed and approved by the Institutional Animal Care and Use Committee of Chiba Cancer Center Research Institute.

Magnetic resonance imaging study. To estimate i.c. tumor volume sequentially, all the animals were examined with magnetic resonance imaging (MRI) every 7 days started on day 7 after the tumor inoculation. Rats were anesthetized with 50 mg/kg pentobarbital and injected with 0.2 mL gandolinium-diethylenetriaminepentaacetic acid (Gd-DTPA, 0.8-1.0 mL/kg). Coronal T_1-weighted images (TR 500 milliseconds, TE 11 milliseconds, 3 mm thickness, gapless) were obtained with a 1.5-T MR device (Signa Advantage, General Electric, Milwaukee, WI). Tumor volume (mm^3) was calculated as the sum of the Gd-DTPA–enhanced portion of each MR-imaged area (mm^2) times the imaged thickness. The estimated tumor volumes on MRI have a linear correlation with actual tumor weights obtained immediately after the imaging study (20).

Immunohistochemistry. Tumor-bearing rats were perfused through the ascending aorta with 4% paraformaldehyde and brains were

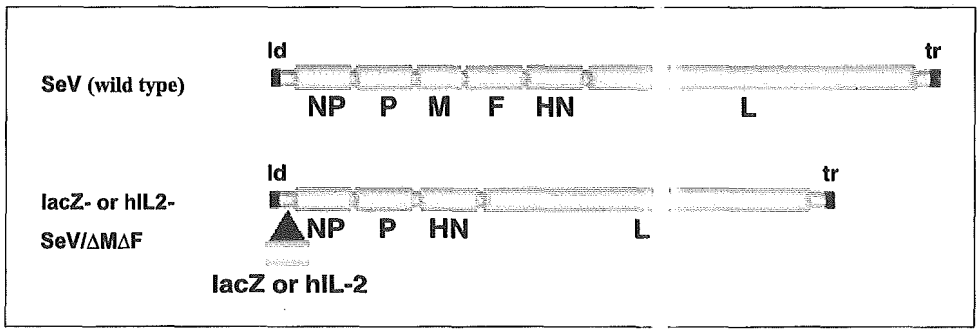

Fig. 1. Schematic genome structures of wild-type SeV and the both *M* and *F* gene – deleted SeV vector carrying *lacZ* or *human IL-2* gene. The open reading frame of the *lacZ* or *human IL-2* gene was inserted with the SeV-specific transcriptional regulatory signal sequences, end and start signals between the leader (*ld*) and the *NP* gene.

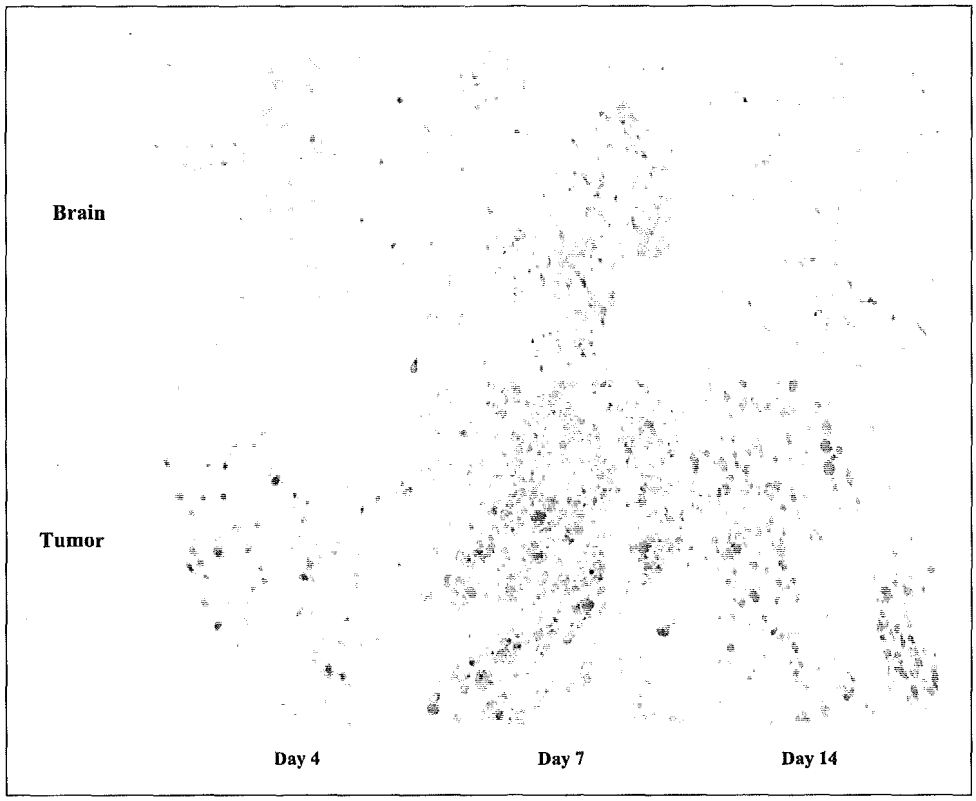

Fig. 2. 5-Bromo-4-chloro-3-indolyl-β-D-galactopyranoside staining of rat brain tissues (*top*) and 9L brain tumors after 7 days of growth in the brain (*bottom*) administered *in situ* with lacZ-SeV/ΔMΔF. Four, seven, and fourteen days after administration of the vector, 5-bromo-4-chloro-3-indolyl-β-D-galactopyranoside staining was done (×200 magnification). Maximal expression or accumulation of β-galactosidase was obtained on day 7 after injection of the vector, and the expression was maintained on day 14 both in the brain tissues and in the brain tumors.

removed. Frozen tissue sections of the brain specimens at 10 μm thickness slices were reacted with anti-CD4 antibody (W3/25, Serotec, Oxford, United Kingdom), anti-CD8 antibody (OX-8, Serotec), and anti-human IL-2 antibody (R&D Systems, Minneapolis, MN). Tissues were then reacted with horseradish peroxidase–conjugated goat anti-mouse IgG and stained with 3,3′-diaminobenzidine tetrahydrochloride (Nichirei, Tokyo, Japan). β-galactosidase expression was detected using β-Galactosidase Staining Kit (Mirus, Madison, WI).

CTL assay. To test lymphocytes for their antitumor cytotoxicity, a standard 4-hour ^{51}Cr release assay was done. Spleen cells (1×10^6 cells) were harvested from rats on day 14 after treatment and were cultured in RPMI 1640 supplemented with 10% FCS and 5×10^{-5} mol/L 2-mercaptoethanol. They were stimulated *in vitro* with irradiated 9L cells for 5 days. Syngeneic 9L or allogeneic C6 cells were used as ^{51}Cr-labeled targets and were cultured with the spleen cells at various effector-to-target cell ratios. After 4-hour incubation, radioactivities in the culture supernatants were counted with an automatic γ-counter. Specific cytotoxic activity was calculated as follows: 100 × ([experimental counts per minute − spontaneous counts per minute] / [maximal counts per minute − spontaneous counts per minute]). The maximal counts per minute were released by adding 1% NP40 to wells in experiments.

Statistics. Comparison of tumor volumes in each treatment group was done with the unpaired *t* test. The Kaplan-Meier method was used to estimate the survival rates and the Cox-mantel log-rank test was used to compare the survival differences in each treatment group. All of the statistical analyses were done with the StatView software (SAS Institute, Inc., Cary, NC).

Results

Sendai virus vector–mediated transduction of β-galactosidase gene into glioma tissue. The efficiency of i.c. transduction of the *β-galactosidase* gene by SeV vector was examined in brain tumors and normal brain tissues removed 4, 7, and 14 days after administration of lacZ-SeV/ΔMΔF. When injected into the brain tumor, the typical appearance of the vector-injected tissues was scattered colonies of 5-bromo-4-chloro-3-indolyl-β-D-galactopyranoside–positive cells, which were composed of transduced tumor cells from the injected lacZ-SeV/ΔMΔF (Fig. 2). Nontransduced tumor cells were seen between the scattered 5-bromo-4-chloro-3-indolyl-β-D-galactopyranoside–stained colonies. Maximal expression or accumulation of

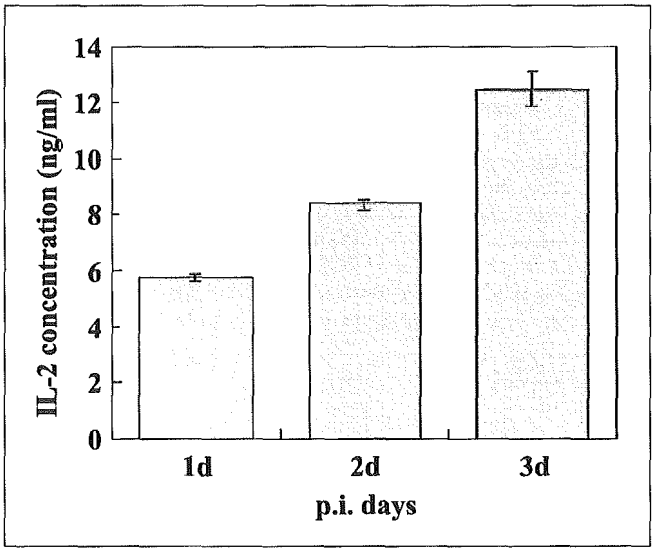

Fig. 3. Kinetics of the expression of IL-2 protein in the cells infected with hIL2-SeV/ΔMΔF *in vitro*. LLC-MK_2 cells (10^6) were infected at a multiplicity of infection of 10 with hIL2-SeV/ΔMΔF. The culture supernatants were collected every 24 hours and the amounts of IL-2 protein were quantified by ELISA. Substantial amount of IL-2 was secreted even at 1 day after the infection. The maximum production of 12.5 ng/mL was observed at day 3.

β-galactosidase was obtained on day 7 and the expression level was maintained on day 14 after injection of the vector. Transduction of normal brain surrounding the tumor was scarcely detected with the exception of the choroid plexus. When injected into the normal brain tissues, transductions of neurons and glial cells were also observed at lower efficiency compared with the case of intratumoral injection. Ependymal cells were not transduced by the intraparenchymal injection of the vector.

In vitro ***kinetics of interleukin-2 production by cells infected with hIL2-SeV/ΔMΔF.*** To clarify the transgene expression induced by hIL2-SeV/ΔMΔF, the amount of IL-2 production by the cells infected with hIL2-SeV/ΔMΔF was investigated by ELISA. Sufficient amount of IL-2 protein (5.8 ng/mL) was detected at day 1 after the vector infection and increased to 12.5 ng/mL at 3 days after the infection (Fig. 3).

Antitumor effects of i.c. administration of hIL2-SeV/ΔMΔF. All the naive rats inoculated with 9L cells in the brain developed progressive tumors. We examined the therapeutic effect of i.c. administration of hIL2-SeV/ΔMΔF combined with s.c. vaccination by measuring the tumor volumes with serial Gd-enhanced MRI (Fig. 4A). The tumor volumes on day 21 in the rats treated with the i.c. administration of hIL2-SeV/ΔMΔF and the vaccination (86.5 ± 63.8 mm^3, $n = 10$) were significantly smaller than the following groups: untreated (286 ± 51.2 mm^3, $n = 10$, $P < 0.0001$); vaccination alone (197 ± 48.9 mm^3, $n = 10$, $P = 0.0005$); i.c. administration of lacZ-SeV/ΔMΔF combined with the vaccination (233 ± 73.2 mm^3, $n = 6$, $P = 0.0012$); and i.c. administration of hIL2-SeV/ΔMΔF alone (256 ± 53.2 mm^3, $n = 6$, $P = 0.0001$; Fig. 4B). When treated with the combination strategy, all the inoculated tumors became visible by MRI on day 21 and the established brain tumors were completely eliminated in 3 of 10 rats (Fig. 4A). There was no difference in the tumor volumes on day 21 between the three cured tumors (81.6 ± 74.9 mm^3) and the other seven tumors (88.6 ± 67.1 mm^3). Accordingly, the lifetime of the rats treated with i.c. administration of hIL2-SeV/ΔMΔF vector combined with the vaccination was significantly prolonged compared with the untreated control rats or the rats treated otherwise ($P < 0.05$, log-rank test; Fig. 4C). All the cured animals completely rejected

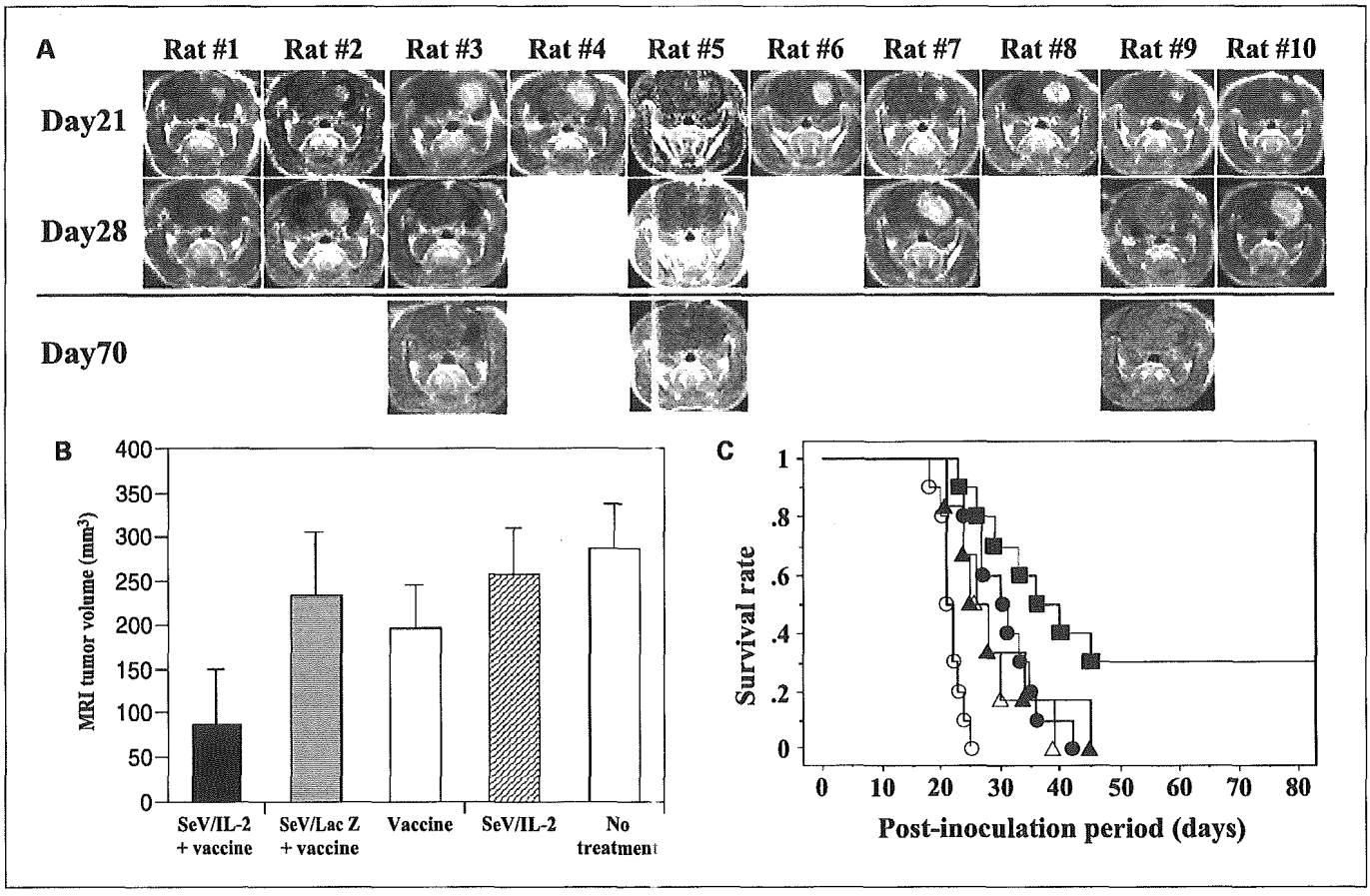

Fig. 4. Antitumor effects of i.c. administration of hIL2-SeV/ΔMΔF. *A*, Gd-DTPA–enhanced MRI images of all the 9L brain tumors treated with i.c. administration of hIL2-SeV/ΔMΔF and s.c. vaccination of irradiated wild-type 9L cells. All the animals were examined with MRI every 7 days, starting on day 7 after tumor inoculation. When treated with the combination strategy, all the i.c. tumors became visible at latest on day 21. The established brain tumors completely disappeared on day 28 in 3 of 10 rats examined (rats 3, 5, and 10). There was no difference in the tumor volumes on day 21 between the three eliminated tumors (81.6 ± 74.9 mm^3) and those of the seven other tumors (88.6 ± 67.1 mm^3). *B*, mean volumes of the 9L brain tumors measured by Gd-enhanced MRI on day 21. I.c. administration of hIL2-SeV/ΔMΔF combined with the vaccination (86.5 ± 63.8 mm^3, $n = 10$) resulted in significantly smaller volumes than the following groups: untreated (286 ± 51.2 mm^3, $n = 10$, $P < 0.0001$), vaccination alone (197 ± 48.9 mm3, $n = 10$, $P = 0.0005$), i.c. administration of lacZ-SeV/ΔMΔF combined with the vaccination (233 ± 73.2 mm^3, $n = 6$, $P = 0.0012$), and i.c. administration of hIL2-SeV/ΔMΔF alone (256 ± 53.2 mm^3, $n = 6$, $P = 0.0001$). Columns, mean; bars, SD. *C*, Kaplan-Meier survival analysis of the tumor-bearing rats. ○, untreated; ●, treated with the vaccination alone; ▲, treated with i.c. administration of lacZ-SeV/ΔMΔF and the vaccination; △, treated with i.c. administration of hIL2-SeV/ΔMΔF alone; ■, treated with i.c. administration of hIL2-SeV/ΔMΔF and the vaccination. Statistical analysis with log-rank test showed that the rats treated with i.c. administration of hIL2-SeV/ΔMΔF and the vaccination survived significantly longer than the other treatment groups ($P < 0.05$).

a second challenge of wild-type 9L inoculation in the brain and manifested no adverse effect during the 3-month follow-up period.

Induction of tumor-specific cytotoxic T cells. We used the standard ^{51}Cr release assay to evaluate the cytotoxic activity of spleen cells from the treated rats or those from naive rats against syngeneic 9L cells or allogeneic C6 cells. The cytotoxicity to 9L targets was strongly induced by the spleen cells from the rats treated with s.c. vaccination of the irradiated wild-type 9L cells (Fig. 5). In contrast, the cytotoxicity of the same effector cells to the C6 targets was not observed. The spleen cells from the tumor-bearing rats that were treated with i.c. administration of hIL2-SeV/ΔMΔF alone did not induce significant cytotoxicity against the 9L cells. These data suggest that the irradiated wild-type 9L cells were sufficiently immunogenic in the peripheral tissue and that the s.c. vaccination with these cells could induce 9L-specific cytotoxic T cells.

Immunohistochemical analysis. To ascertain the gene expression at protein level, we analyzed the immunoreactivity of IL-2 protein in the hIL2-SeV/ΔMΔF-injected tumors and confirmed that IL-2 protein was diffusely expressed in the treated tumors (Fig. 6A). We also immunohistochemically examined the presence of $CD4^+$ T cells and $CD8^+$ T cells in the tumors. Diffuse and dense infiltrations of $CD4^+$ T cells and $CD8^+$ T cells were observed in the tumors that were treated with i.c. administration of the hIL2-SeV/ΔMΔF and concurrent s.c. vaccination (Fig. 6B). In the tumors treated either with i.c. administration of the lacZ-SeV/ΔMΔF and the vaccination or i.c. administration of the hIL2-SeV/ΔMΔF alone, infiltrations of these cells were sparsely detected.

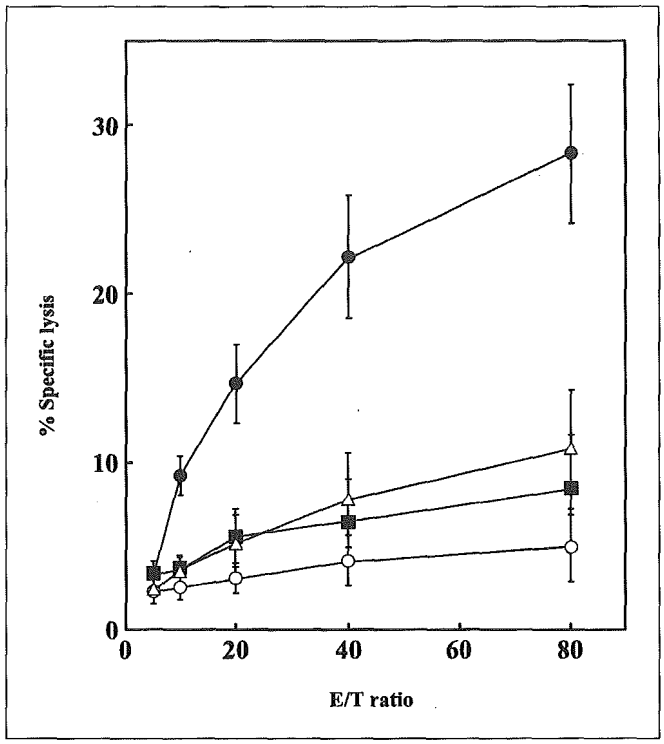

Fig. 5. Cytolytic activity by spleen cells from the treated rats was assessed with a standard ^{51}Cr-release assay against syngeneic 9L or allogeneic C6 targets. ○, spleen cells from naive rats against 9L targets; ●, spleen cells from the rats s.c. vaccinated with irradiated 9L against 9L targets; ■, spleen cells from the vaccinated rats against C6 targets. △, spleen cells from rats treated with i.c. administration of hIL2-SeV/ΔMΔF alone. The vaccination with irradiated 9L cells could induce 9L-specific cytotoxic T cells.

Discussion

We herein first showed that the nontransmissible recombinant SeV vector could transfer genes efficiently into the glioma cells *in vivo*, and this directly correlated with the therapeutic efficacy against the established brain tumors. Even complete elimination of the established brain tumors could be achieved in some cases by the gene therapy strategy using i.c. administration of SeV vector carrying *human IL-2* gene with s.c. vaccination. The SeV vector provided substantive expression of IL-2 protein in the glioma tissues, which would have reached a level necessary to induce significant proliferation and expansion of the peripherally activated tumor-specific T cells.

We have previously reported that transplantation of the IL-2-producing cells into glioma tissues could eliminate approximately half of the established brain tumors in animals immunized with an irradiated whole tumor cell vaccine (16). Although the amount of IL-2 produced by the cells transduced with hIL2-SeV/ΔMΔF was several times greater than that of the IL-2-producing cells utilized in the previous experiment, the cellular infiltration and the cure rate obtained with the hIL2-SeV/ΔMΔF treatment were comparable with those of the cell-mediated therapy. This result would partly be explained by the kinetics of the IL-2 expression in the animals treated with hIL2-SeV/ΔMΔF. The *in vivo* protein expression would have reached its peak 4 days or later after injection of the vector. However, because the tumor doubling time of human glioblastoma is presumed to be longer than the experimental 9L gliosarcoma model, the time lag to reach maximum IL-2 production is not considered to be a critical factor in clinical practice (21). In contrast, the main advantage of virus vector application would be the wide distribution of the transgene products achieved by a small amount of viral solution to be i.c. injected compared with the cell-mediated therapy that needs a large amount of therapeutic cells to cover the whole tumor areas in the human brain.

For the clinical application of this strategy, it would be important to verify the reasons for the difference in the therapeutic efficacy of hIL2-SeV/ΔMΔF among individual animals. This experimental brain tumor model using 9L cells has a quite stable property; the animals are 100% fatal between 18 and 25 days after inoculation and all the untreated tumors are visible by MRI on day 7 with a mean size of 8.0 ± 6.0 mm^3 (16, 17). When treated with hIL2-SeV/ΔMΔF and the vaccination, the observed tumor volumes on day 21 were not different between the eliminated tumors and the other progressing tumors. The pretreatment status of the tumors is not considered to affect the therapeutic outcome. Instead, the presumable differences in the vector injection site (i.e., the center or periphery of the tumor) would affect the efficacy because the stereotactic coordinates used for the tumor inoculation would not necessarily indicate the center of the established tumor. When used in clinical practice, we can precisely identify the center of the brain tumors by computed tomography-guided stereotactic apparatus or navigation system. Another important factor contributing to the difference in therapeutic efficacy may be the expression level of sialic acids.